Quasi-One-Dimensional Bose Gases with a Large Scattering Length

G. E. Astrakharchik,[1,2] D. Blume,[3] S. Giorgini,[1] and B. E. Granger[4]
[1]*Dipartimento di Fisica, Università di Trento and BEC-INFM, I-38050 Povo, Italy*
[2]*Institute of Spectroscopy, 142190 Troitsk, Moscow region, Russia*
[3]*Department of Physics, Washington State University, Pullman, Washington 99164-2814, USA*
[4]*Institute for Theoretical Atomic, Molecular and Optical Physics, Harvard-Smithsonian CFA, Cambridge, Massachusetts 02138, USA*
(Received 28 August 2003; published 22 January 2004)

Bose gases confined in highly elongated harmonic traps are investigated over a wide range of interaction strengths using quantum Monte Carlo techniques. We find that the properties of a Bose gas under tight transverse confinement are well reproduced by a 1D model Hamiltonian with contact interactions. We point out the existence of a unitary regime, where the properties of the quasi-1D Bose gas become independent of the actual value of the 3D scattering length a_{3D}. In this unitary regime, the energy of the system is well described by a hard-rod equation of state. We investigate the stability of quasi-1D Bose gases with positive and negative a_{3D}.

DOI: 10.1103/PhysRevLett.92.030402 PACS numbers: 03.75.Hh, 03.75.Kk

In recent years the study of quasi-1D quantum Bose gases has attracted a great deal of interest. Intriguing properties of quasi-1D gases, such as the exact mapping between interacting bosons and noninteracting fermions, have been predicted [1–3]. A bosonic gas that behaves as if it consisted of spinless fermions, a so-called Tonks-Girardeau (TG) gas, cannot be described within mean-field theory since it exhibits strong correlations; instead, a many-body framework is called for. While experimental evidence of quasi-1D behavior has been reported for bosonic atomic gases under highly elongated harmonic confinement [4], TG gases have not been observed yet. It has been suggested, however, that TG gases can be realized experimentally for either low atomic densities or strong atom-atom interaction strengths. The 3D *s*-wave scattering length a_{3D}, and hence the strength of atom-atom interactions, can be tuned to essentially any value, including zero and $\pm\infty$, by utilizing a magnetic atom-atom Feshbach resonance [5,6].

Utilizing a two-body Feshbach resonance, 3D degenerate gases with large scattering length a_{3D} have been studied experimentally and theoretically. For $a_{3D} \to \pm\infty$, it is predicted that the behavior of the strongly correlated gas is independent of a_{3D} [7]. For *homogeneous* 3D Bose gases, this unitary regime can most likely not be reached experimentally since three-body recombination is expected to set in when a_{3D} becomes comparable to the average interparticle distance. Three-body recombination leads to cluster formation, and hence "destroys" the gas-like state. The situation is different for Fermi gases, for which the unitary regime has already been achieved experimentally [6]. In this case, the Fermi pressure stabilizes the system even for large $|a_{3D}|$. It has been predicted that three-body recombination processes are suppressed for strongly interacting 1D Bose gases [8]. These studies raise the question whether a *highly elongated inhomogeneous* Bose gas, that is, an inhomogeneous quasi-1D Bose gas, is stable as $a_{3D} \to \pm\infty$.

This Letter investigates the properties of a quasi-1D Bose gas at zero temperature over a wide range of interaction strengths within a microscopic, highly accurate many-body framework. We find that the system (i) is well described by a 1D model Hamiltonian with contact interactions and renormalized coupling constant [2] for any value of the 3D scattering length a_{3D}; (ii) behaves like a TG gas for a critical positive value of a_{3D}; (iii) reaches a unitary regime for large values of $|a_{3D}|$, where the properties of the quasi-1D Bose gas become independent of the actual value of a_{3D} and are similar to those of a hard-rod gas; and (iv) becomes unstable against cluster formation for a critical negative value of a_{3D}.

Our study is based on the 3D Hamiltonian H_{3D},

$$H_{3D} = \sum_{i=1}^{N}\left[\frac{-\hbar^2}{2m}\nabla_i^2 + \frac{m}{2}(\omega_\rho^2\rho_i^2 + \omega_z^2 z_i^2)\right] + \sum_{i<j} V(r_{ij}), \quad (1)$$

which describes N spin-polarized mass m bosons under highly elongated confinement with $\omega_z = \lambda\omega_\rho$, where $\lambda \ll 1$. The coordinates $\rho_i = \sqrt{x_i^2 + y_i^2}$ and z_i denote, respectively, the radial and the axial position of the ith particle, $r_{ij} = |\vec{r}_i - \vec{r}_j|$ denotes the interparticle distance between atom i and j, and $V(r)$ denotes the two-body interatomic potential. We consider two different potentials: (i) a purely repulsive hard-sphere (HS) potential, $V^{HS}(r) = \infty$ for $r < a_{3D}$, and zero otherwise and (ii) a more realistic short-range (SR) potential, which can support two-body bound states, $V^{SR}(r) = -V_0/\cosh^2(r/r_0)$, with well depth V_0. For V^{HS}, the s-wave scattering length a_{3D} coincides with the range of the potential. For V^{SR}, in contrast, r_0 determines the range of the potential, while the scattering length a_{3D} is a function of r_0 and V_0. In our calculations, r_0 is fixed at a value much smaller than the transverse oscillator length, $r_0 = 0.1a_\rho$, where $a_\rho = \sqrt{\hbar/m\omega_\rho}$. To simulate the behavior of a_{3D} near a field-dependent Feshbach resonance, we vary the well depth V_0 and consequently the scattering length a_{3D}. Importantly, a_{3D} diverges for particular values of V_0 (the inset of Fig. 1 shows one such divergence). At each divergence, a new two-body s-wave bound state is pulled in. Our numerical calculations (see below) are performed for the well depths V_0 shown in the inset of Fig. 1.

We consider situations where the bosonic gas described by Eq. (1) is in the 1D regime for any value of the 3D scattering length a_{3D}, which implies $N\lambda \ll 1$. If the range of $V(r)$ is much smaller than a_ρ, it is predicted [2] that the properties of the 3D gas are well described by the 1D contact-interaction Hamiltonian H_{1D},

$$H_{1D} = \sum_{i=1}^{N}\left(\frac{-\hbar^2}{2m}\frac{\partial^2}{\partial z_i^2} + \frac{m}{2}\omega_z^2 z_i^2\right) + g_{1D}\sum_{i<j}\delta(z_{ij}) + N\hbar\omega_\rho, \tag{2}$$

where g_{1D} is an effective coupling constant. The limit $g_{1D} \to 0$ corresponds to the weakly interacting mean-field regime, while $g_{1D} \to \infty$ corresponds to the strongly interacting TG regime. For positive g_{1D} and vanishing confinement ($\omega_\rho = \omega_z = 0$), Eq. (2) reduces to the Lieb-Liniger (LL) Hamiltonian [9], whose gaslike properties have been studied in detail. For negative g_{1D} and $\omega_\rho = \omega_z = 0$, Eq. (2) supports clusterlike bound states [10]; little is known about gaslike states in this case.

Below, we solve the many-body Schrödinger equation for the 1D Hamiltonian *with confinement*, Eq. (2), for positive *and* negative g_{1D}, and relate our results to those for the 3D Hamiltonian, Eq. (1). Considering two bosons in a highly elongated geometry that interact through a regularized zero-range pseudopotential, Olshanii [2] shows that the effective 1D coupling constant g_{1D} can be expressed in terms of the known 3D scattering length a_{3D},

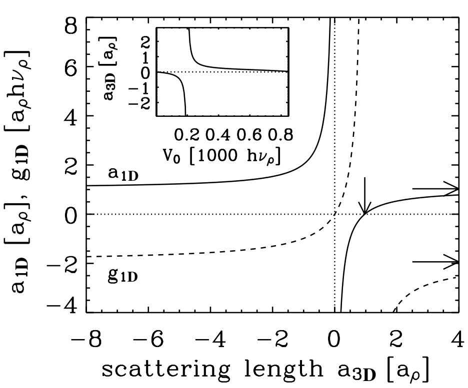

FIG. 1. g_{1D} [dashed line, Eq. (3)] and a_{1D} [solid line, Eq. (4)] as a function of a_{3D}. A vertical arrow indicates the value of a_{3D} where g_{1D} diverges, $a_{3D}^c/a_\rho = 0.9684$. Horizontal arrows indicate the asymptotic values of g_{1D} and a_{1D}, respectively, as $a_{3D} \to \pm\infty$ ($g_{1D} = -1.9368a_\rho\hbar\omega_\rho$ and $a_{1D} = 1.0326a_\rho$). Inset: a_{3D} as a function of the well depth V_0 for $V^{SR}(r)$.

$$g_{1D} = \frac{2\hbar^2 a_{3D}}{m a_\rho^2}\frac{1}{1 - A a_{3D}/a_\rho}, \tag{3}$$

where $A = |\zeta(1/2)|/\sqrt{2} = 1.0326$. Alternatively, g_{1D} can be expressed through the effective 1D scattering length a_{1D}, $g_{1D} = -2\hbar^2/(m a_{1D})$ [2], where

$$a_{1D} = -a_\rho\left(\frac{a_\rho}{a_{3D}} - A\right). \tag{4}$$

For $a_{3D} > 0$ (but $a_{3D} \ll a_\rho$), g_{1D} approaches the unrenormalized coupling constant, $g_{1D}^0 = 2\hbar^2 a_{3D}/(m a_\rho^2)$, which is obtained by averaging the 3D coupling constant $g_{3D} = 4\pi\hbar^2 a_{3D}/m$ over the transverse oscillator ground state (see, e.g., Ref. [3]). For these values of a_{3D}, the 1D Hamiltonian given in Eq. (2) with g_{1D} replaced by g_{1D}^0 describes a quasi-1D system accurately [11].

For $a_{3D} \gtrsim a_\rho$ and for negative a_{3D}, in contrast, the confinement induced renormalization becomes important, and the effective 1D coupling constant g_{1D} and scattering length a_{1D}, Eqs. (3) and (4), have to be used. Figure 1 shows g_{1D} (dashed line) and a_{1D} (solid line) as a function of a_{3D}. At the critical value $a_{3D}^c = 0.9684a_\rho$ (indicated by a vertical arrow in Fig. 1), g_{1D} diverges while a_{1D} goes through zero. At the 3D resonance, that is, for $a_{3D} \to \pm\infty$, g_{1D} and a_{1D} each reach an asymptotic value ($g_{1D} = -1.9368a_\rho\hbar\omega_\rho$ and $a_{1D} = 1.0326a_\rho$, respectively, indicated by horizontal arrows in Fig. 1). Tuning a_{3D} to large values hence allows a unitary quasi-1D regime, where g_{1D} and a_{1D} are independent of a_{3D}, to be entered.

We solve the Schrödinger equation for the many-body 3D Hamiltonian, Eq. (1), numerically using the diffusion quantum Monte Carlo (DMC) technique. Our interest is in the lowest gaslike many-body state. For V^{HS}, the lowest gaslike state of H_{3D} coincides with the many-body ground state; to describe this state we can hence use the "standard" DMC technique (see, e.g., [12]). For V^{SR}, in contrast, the many-body ground state is a clusterlike bound state. To describe the lowest-lying gaslike state, i.e., an excited state, we hence use the fixed-node DMC (FN-DMC) method [13]. For a given many-body nodal surface, the FN-DMC method allows the Schrödinger equation to be solved for approximate excited states. For $N = 2$, we obtain the exact nodal surface by direct diagonalization. Assuming that the scattering properties between each atom pair are unaltered by the presence of other atoms, we then use the $N = 2$ nodal surface to construct the many-body nodal surface. For dilute quasi-1D gases we expect that the FN-DMC approach as implemented here results in highly accurate many-body energies.

Figure 2 shows the resulting 3D energy per particle, $E/N - \hbar\omega_\rho$, as a function of a_{3D} for $N = 5$ under quasi-1D confinement, $\lambda = 0.01$, for the hard-sphere and the short-range two-body potential, V^{HS} (diamonds) and V^{SR} (asterisks), respectively. For small a_{3D}/a_ρ, the energies

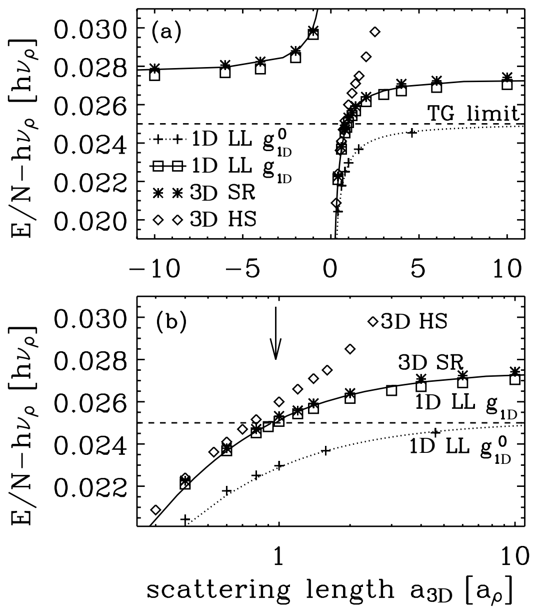

FIG. 2. 3D DMC energy per particle calculated using $V^{\rm HS}$ (diamonds) and $V^{\rm SR}$ (asterisks), respectively, together with 1D DMC energy per particle calculated using g_{1D} [squares, Eq. (3)] and g^0_{1D} (plusses), respectively, as a function of a_{3D} [(a) linear scale; (b) logarithmic scale] for $N = 5$ and $\lambda = 0.01$. The statistical uncertainty of the DMC energies is smaller than the symbol size. Dotted and solid lines show the 1D energy per particle calculated within the local density approximation (LDA) for g^0_{1D} (using the LL equation of state) and for g_{1D}, Eq. (3) (using the LL equation of state for $g_{1D} > 0$, and the hard-rod (HR) equation of state for $g_{1D} < 0$), respectively. A dashed horizontal line indicates the TG energy, and a vertical arrow the position where g_{1D}, Eq. (3), diverges.

for these two two-body potentials agree within the statistical uncertainty. For $a_{3D} \gtrsim a_\rho$, however, clear discrepancies are visible. The DMC energies for $V^{\rm SR}$ cross the TG energy per particle (indicated by a dashed horizontal line), $E/N - \hbar\omega_\rho = \hbar\omega_\rho \lambda N/2$, very close to the value $a^c_{3D} = 0.9684 a_\rho$ [indicated by a vertical arrow in Fig. 2(b)], while the energies for $V^{\rm HS}$ cross the TG energy per particle at a notably smaller value of a_{3D}.

To compare our results obtained for the 3D Hamiltonian, H_{3D}, with those for the 1D Hamiltonian, H_{1D}, we also solve the Schrödinger equation for H_{1D}, Eq. (2). For positive values of the coupling constant g_{1D} we calculate the many-body ground state energy by the exact DMC method. For $g_{1D} < 0$, however, the 1D Hamiltonian supports many-body bound states, and, as in the 3D case, we use the FN-DMC method to describe the lowest-lying gaslike state. For $N = 2$ and $g_{1D} < 0$, the first excited state of the Schrödinger equation for H_{1D}, Eq. (2), has a node at $z_{12} = a_{1D}$. To solve the many-body Schrödinger equation for H_{1D} with negative g_{1D} for the lowest gaslike state by the FN-DMC technique, we parametrize our many-body nodal surface in terms of a_{1D}. This many-body nodal surface is expected to be good if the density of the gas is low.

In addition to the 3D energy per particle, Fig. 2 shows the resulting 1D energy per particle obtained by solving the Schrödinger equation for H_{1D}, Eq. (2), for the renormalized coupling constant g_{1D} [squares, Eq. (3)], and the unrenormalized coupling constant g^0_{1D} (plusses), respectively. The 1D energies calculated using the two different coupling constants agree well for small a_{3D}, while clear discrepancies become apparent for larger a_{3D}. Importantly, the 1D energies calculated using the renormalized 1D coupling constant g_{1D} agree well with the 3D energies calculated using the short-range potential $V^{\rm SR}$ (asterisks) up to very large values of the 3D scattering length a_{3D}, and also for negative a_{3D}. In contrast, at large a_{3D} the 1D energies deviate clearly from the 3D energies calculated using the hard-sphere potential $V^{\rm HS}$ (diamonds). We conclude that the renormalization of the effective 1D coupling constant g_{1D} and the 1D scattering length a_{1D} are crucial to reproduce the results of the 3D Hamiltonian H_{3D} when $a_{3D} \gtrsim a_\rho$ and when a_{3D} is negative. Small deviations between the 1D energies calculated using the renormalized 1D coupling constant g_{1D} and the 3D energies calculated using the short-range potential $V^{\rm SR}$ remain; we attribute these to the finite range of $V^{\rm SR}$.

If the size of the cloud is much larger than the harmonic oscillator length a_z, where $a_z = \sqrt{\hbar/m\omega_z}$, it has been shown that the properties of the 1D LL Hamiltonian H_{1D}, $g_{1D} > 0$, are well described by a simple equation of state using the LDA [14]. For $g_{1D} < 0$, we instead apply the equation of state for 1D HRs. Recall that the many-body nodal surface of the lowest-lying gaslike state of H_{1D} with $g_{1D} < 0$ is well parametrized by a_{1D}. For $z_{ij} > a_{1D}$, the corresponding wave function coincides with that of N 1D hard rods of size a_{1D}. For small values of the 1D gas parameter, $n_{1D} a_{1D} \ll 1$, where n_{1D} denotes the linear density, we hence expect that the lowest-lying gaslike state of the 1D many-body Hamiltonian with $g_{1D} < 0$ is well described by a system of hard rods of size a_{1D}. The exact energy per particle of the uniform hard-rod system is given by $E/N = (\pi^2\hbar^2 n^2_{1D}/6m)/(1 - n_{1D}a_{1D})^2$ [1]. For trapped systems with $N\lambda \ll 1$ we obtain the expansion

$$E/N - \hbar\omega_\rho = \hbar\omega_\rho \frac{N\lambda}{2}\left(1 + \frac{128\sqrt{2}}{45\pi^2}\sqrt{N\lambda}\frac{a_{1D}}{a_\rho} + \cdots\right). \tag{5}$$

The first term corresponds to the energy per particle in the TG regime. Similarly, the linear density in the center of the cloud is to lowest order given by the TG result, $n_{1D} = \sqrt{2N\lambda}/(\pi a_\rho)$. In the unitary limit, that is, for $a_{1D}/a_\rho = 1.0326$, expression (5) becomes independent of a_{3D} and depends only on $N\lambda$.

Lines in Fig. 2 show the resulting 1D energies per particle for the LL equation of state ($g_{1D} > 0$) as well as for the HR equation of state ($g_{1D} < 0$) calculated within the LDA. Remarkably, the LDA energies nearly coincide with the 1D many-body DMC energies (plusses and squares, respectively); finite-size effects play a role only for $a_{3D} \ll a_\rho$. Our calculations establish for the first time that a simple treatment, i.e., a HR equation of state treated within the LDA, describes trapped quasi-1D gases with negative coupling constant g_{1D} well over a wide range of the 3D scattering length a_{3D}. For $a_{3D} \rightarrow ^{-}0$, that is, for large a_{1D}, the HR equation of state using the LDA cannot properly describe trapped quasi-1D gases, which are expected to become unstable against formation of clusterlike many-body bound states for $a_{1D} \approx 1/n_{1D}$. We hence investigate the regime with negative a_{3D} in more detail within a many-body framework.

By comparing with results for the 3D Hamiltonian, Eq. (1), we have shown above that the 1D Hamiltonian H_{1D}, Eq. (2), provides an excellent description of quasi-1D gases. We hence base our stability analysis of quasi-1D gases with large effective 1D scattering length a_{1D} on H_{1D}. We solve the many-body Schrödinger equation for H_{1D} using the variational quantum Monte Carlo (VMC) method. Our variational N-particle Bijl-Jastrow–type wave function consists of one- and two-body terms. The one-body terms are written as a function of a single variational parameter α, which determines the size of the atomic gas. The two-body term is parametrized by a_{1D} and explicitly accounts for correlations.

Figure 3 shows the resulting VMC energy per particle for $N = 5$ and $\lambda = 0.01$ as a function of the variational parameter α (Gaussian width) for four different a_{1D}. For $a_{1D}/a_\rho = 1$ and 2, Fig. 3 shows a local minimum at $\alpha_{\min} \approx a_z$. The minimum VMC energy nearly coincides with the essentially exact DMC energy, which suggests that our variational wave function provides a highly accurate description of the quasi-1D many-body system. The energy barrier at $\alpha \approx 0.2a_z$ decreases with increasing a_{1D} and disappears for $a_{1D}/a_\rho \approx 3$. We interpret this vanishing of the energy barrier as an indication of instability [15]. For small a_{1D}, the energy barrier separates the gaslike state from clusterlike bound states. For larger a_{1D}, this energy barrier disappears and the gaslike state becomes unstable against cluster formation.

We additionally performed variational calculations for larger N and different λ. We find that the onset of instability of quasi-1D Bose gases can be described by the product of the 1D scattering length a_{1D} and the linear density at the trap center n_{1D}. To be specific, our many-body calculations suggest that a quasi-1D gas is stable for $a_{1D}n_{1D} \lesssim 0.35$ and becomes unstable for $a_{1D}n_{1D} \gtrsim 0.35$. Our analysis suggests that the quasi-1D unitary regime can be reached experimentally. By tuning the 3D scattering length, it is further possible to investigate the onset of instability. By reducing λ one should be able to stabilize relatively large quasi-1D systems.

In conclusion, we investigated the energetics of a Bose gas under highly elongated harmonic confinement over a wide range of the 3D scattering length. We find that the quasi-1D gas can be described by a many-body 1D model Hamiltonian with zero-range interactions and renormalized coupling constant. For $a_{3D} \rightarrow \pm\infty$, the quasi-1D gas enters a unitary regime, where all properties of the system are independent of a_{3D}. In the vicinity of the unitary regime, the quasi-1D system behaves like a gas of HRs. For negative a_{3D}, quasi-1D gases become unstable against cluster formation for a critical value of $a_{1D}n_{1D}$.

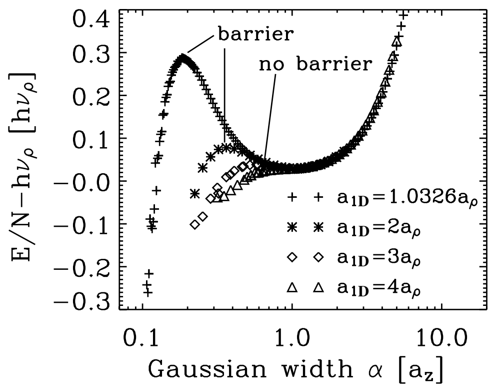

FIG. 3. VMC energy per particle as a function of the variational parameter α for $N = 5$, $\lambda = 0.01$, and $a_{1D}/a_\rho = 1.0326$ (plusses), 2 (asterisks), 3 (diamonds), and 4 (triangles).

G. E. A. and S. G. acknowledge support by the Ministero dell'Istruzione, dell'Università e della Ricerca (MIUR). D. B. acknowledges support by the NSF (Grant No. 0331529) and by the BEC Center at the University of Trento, and B. E. G. by the NSF through a grant to ITAMP.

[1] M. Girardeau, J. Math. Phys. (N.Y.) **1**, 516 (1960).
[2] M. Olshanii, Phys. Rev. Lett. **81**, 938 (1998).
[3] D. S. Petrov, G. V. Shlyapnikov, and J. T. M. Walraven, Phys. Rev. Lett. **85**, 3745 (2000).
[4] A. Görlitz *et al.*, Phys. Rev. Lett. **87**, 130402 (2001); F. Schreck *et al.*, *ibid.* **87**, 080403 (2001); M. Greiner *et al.*, *ibid.* **87**, 160405 (2001).
[5] S. Inouye *et al.*, Nature (London) **392**, 151 (1998); S. L. Cornish *et al.*, Phys. Rev. Lett. **85**, 1795 (2000); T. Loftus *et al.*, Phys. Rev. Lett. **88**, 173201 (2002).
[6] K. M. O'Hara *et al.*, Science **298**, 2179 (2002); T. Bourdel *et al.*, Phys. Rev. Lett. **91**, 020402 (2003).
[7] S. Cowell *et al.*, Phys. Rev. Lett. **88**, 210403 (2002); H. Heiselberg, Phys. Rev. A **63**, 043606 (2001).
[8] D. M. Gangardt and G. V. Shlyapnikov, Phys. Rev. Lett. **90**, 010401 (2003).
[9] E. H. Lieb and W. Liniger, Phys. Rev. **130**, 1605 (1963); E. H. Lieb, *ibid.* **130**, 1616 (1963).
[10] J. B. McGuire, J. Math. Phys. (N.Y.) **5**, 622 (1964).
[11] D. Blume, Phys. Rev. A **66**, 053613 (2002); G. E. Astrakharchik and S. Giorgini, *ibid.* **66**, 053614 (2002).
[12] J. Boronat and J. Casulleras, Phys. Rev. B **49**, 8920 (1994).
[13] P. J. Reynolds, D. M. Ceperley, B. J. Alder, and W. A. Lester, Jr., J. Chem. Phys. **77**, 5593 (1982).
[14] V. Dunjko, V. Lorent, and M. Olshanii, Phys. Rev. Lett. **86**, 5413 (2001).
[15] J. L. Bohn, B. D. Esry, and C. H. Greene, Phys. Rev. A **58**, 584 (1998); H. T. C. Stoof, J. Stat. Phys. **87**, 1353 (1997).